



PAPER

Cone-beam computed tomography-based delta-radiomics for early response assessment in radiotherapy for locally advanced lung cancer

Litong Shi^{1,2,4}, Yi Rong^{1,4} , Megan Daly¹, Brandon Dyer¹, Stanley Benedict¹, Jianfeng Qiu^{2,3,5} and Tokihiro Yamamoto^{1,5} 

¹ Department of Radiation Oncology, University of California Davis School of Medicine, Sacramento, CA 95817, United States of America

² Medical Engineering and Technology Research Center; Imaging-X Joint Laboratory; Department of Radiology, Shandong First Medical University and Shandong Academy of Medical Sciences, Taian 271016, People's Republic of China

³ Shandong First Medical University and Shandong Academy of Medical Sciences, No. 619, Changcheng Road, Taian, Shandong 271016, People's Republic of China

⁴ LS and YR contributed equally to the study.

⁵ Authors to whom any correspondence should be addressed.

E-mail: toyamamoto@ucdavis.edu and jfqi100@gmail.com

Keywords: cone-beam computed tomography (CBCT), delta-radiomics, early response assessment, non-small cell lung cancer

Supplementary material for this article is available [online](#)

Abstract

Cone-beam computed tomography (CBCT) images acquired during radiotherapy may allow early response assessment. Previous studies have reported inconsistent findings on an association of CBCT-measured tumor volume changes with clinical outcomes. The purpose of this pilot study was twofold: (1) to characterize changes in CBCT-based radiomics features during treatment; and (2) to quantify the potential association of CBCT-based delta-radiomics features with overall survival in locally advanced lung cancer.

We retrospectively identified 23 patients and calculated 658 radiomics features from each of 11 CBCT images per patient. Feature selection was performed based on repeatability, robustness against contouring uncertainties, and non-redundancy. We calculated the coefficient of determination (R^2) for the relationship between the actual feature value at the end of treatment and predicted value based on linear models fitted using features between the first and k th fractions. We also quantified the predictive ability for survival with two methods by: (1) comparing delta-radiomics features (defined as the mean change between the first and k th fractions) between two groups of patients divided by a cutoff survival time of 18 months using the t -test or Wilcoxon rank-sum test; and (2) quantifying univariate discrimination of two groups divided by the median of delta-radiomics feature.

All selected seven radiomics features during treatment (as early as the 10th fraction) were predictive of those at the end of treatment ($R^2 > 0.64$). Three delta-radiomics features demonstrated significant differences ($q < 0.05$, as early as the 10th fraction) between the two groups of patients divided by the cutoff survival time. Two of those three features were also predictive of survival according to the log-rank statistics.

We provided the first demonstration of a potential association of CBCT-based delta-radiomics features early during treatment with overall survival in locally advanced lung cancer. Our preliminary findings should be validated for a larger cohort of patients.

RECEIVED
23 April 2019

REVISED
10 July 2019

ACCEPTED FOR PUBLICATION
15 July 2019

PUBLISHED
10 January 2020

Introduction

Lung cancer is the second most common cancer and the leading cause of cancer death in both men and women in the US (Kupelian *et al* 2005, Smith *et al* 2018). For locally advanced inoperable lung cancer, chemotherapy combined with fractionated radiotherapy is a common treatment regimen that can improve survival rates compared to radiation therapy alone (Molina *et al* 2008). However, between 2008 and 2014, the 5 year survival rate for lung cancer patients was only 18.6% (Kupelian *et al* 2005). Early response assessment during a course of treatment could potentially allow response-adapted therapy (i.e. biologically adaptive radiation therapy), which may improve clinical outcomes. For example, the radiation dose could be escalated to nonresponding tumors without increasing the dose to normal tissues through adapting the treatment plan to changing anatomy (Guckenberger *et al* 2011).

Cone-beam computed tomography (CBCT) images, which are commonly used for patient positioning and target localization before each fraction of radiotherapy, may allow early response assessment. Tumor volume changes have been regarded as an important metric to assess treatment response (Dubben *et al* 1998, Mozley *et al* 2012). Previous studies investigated the potential of tumor volume reduction measured on CBCT images in predicting treatment response and clinical outcomes for lung cancer; however, the findings were inconsistent and inconclusive (Brink *et al* 2014, Jabbour *et al* 2015, Mazzola *et al* 2016, Wen *et al* 2017). Jabbour *et al* noted that patients with greater tumor volume reduction survived longer than patients with smaller volume reduction (Jabbour *et al* 2015), while Brink *et al* found that patients with greater tumor volume reduction was associated with poorer survival (Brink *et al* 2014).

Radiomics is an emerging technology to extract vast quantitative features from medical images and has been demonstrated to have significant predictive power for gene expression, response to therapy, and clinical outcomes (Kumar *et al* 2012, Lambin *et al* 2012, Mattonen *et al* 2014, Huynh *et al* 2016, Fave *et al* 2017). Radiomics features extracted from CBCT images may allow for more accurate prediction of treatment response and outcomes compared to tumor volume changes. A recent study found that some radiomics features extracted from CBCT images of the first fraction of treatment were interchangeable with those from planning CT images (van Timmeren *et al* 2017b). Moreover, changes in CBCT-based radiomics were detectable as early as the second week of treatment (van Timmeren *et al* 2017a). These results indicate the feasibility of CBCT-based delta-radiomics. No studies have investigated the prognostic value of CBCT-based delta-radiomics during a course of treatment.

The purpose of this pilot study was twofold: firstly, to characterize changes in CBCT-based radiomics features during a course of treatment; and secondly, to quantify the potential association of CBCT-based delta-radiomics features with overall survival in locally advanced lung cancer.

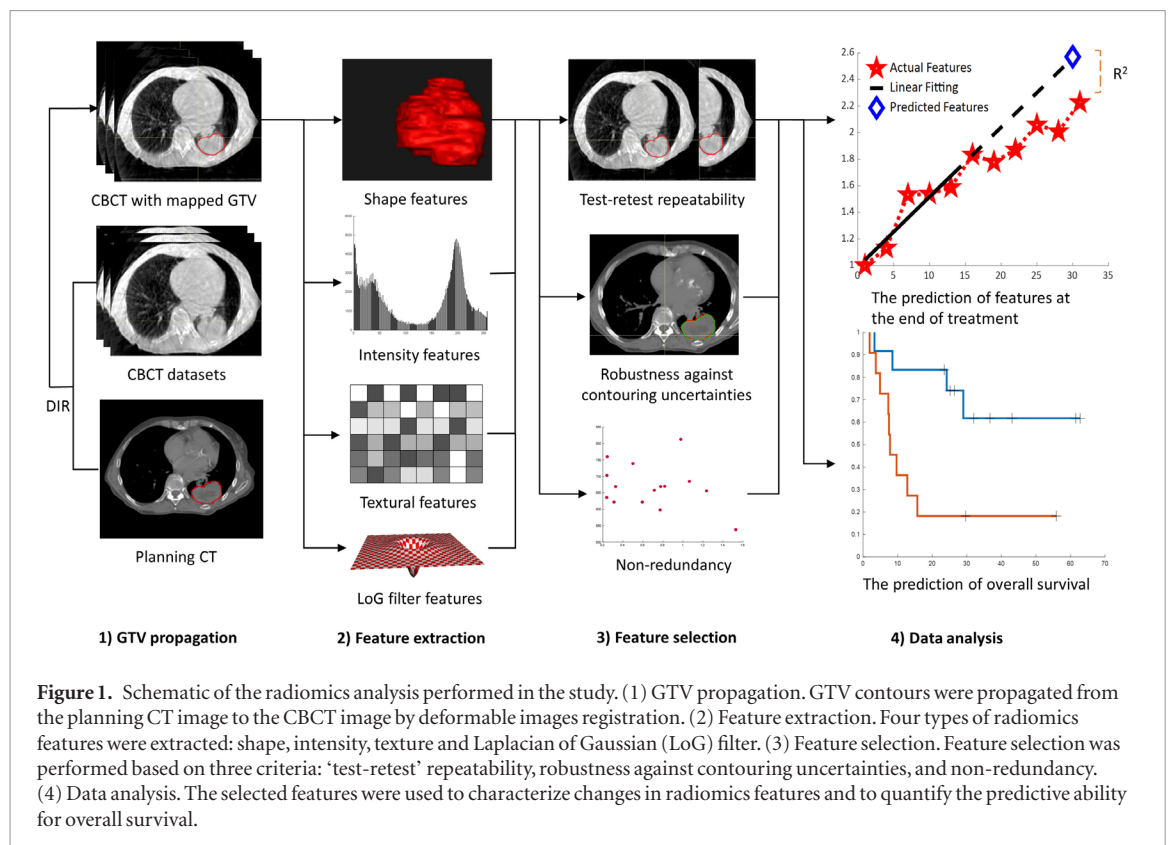
Methods

Patients and image datasets

This study retrospectively reviewed 67 patients with stage III (American Joint Committee on Cancer) non-small cell lung cancer (NSCLC) treated with radiotherapy and concurrent chemotherapy at the University of California Davis between 2011 and 2016 under institutional review board (IRB) approval. Inclusion criteria included: (1) patients received ≥ 58 Gy in 2 Gy daily fractions, (2) patients underwent daily CBCT imaging with consistent acquisition/reconstruction parameters, and (3) patients were followed for at least 18 months or deceased. Patients were excluded if they received prior or subsequent radiotherapy to the thorax, or if the primary tumor and involved lymph nodes were not in the CBCT field of view. A total of 23 patients met the criteria and were included in this study. Supplementary table 1 (stacks.iop.org/PMB/65/015009/mmedia) shows the eligible patients' clinical characteristics. CBCT image datasets were selected at an interval of 3 ± 1 fractions, resulting in a total of 11 image datasets per patient. A time window of ± 1 fraction was used to maintain intra-patient consistency in the following image acquisition/reconstruction parameters: tube voltage (kVp), tube current (mA), exposure time, pixel size, slice thickness, and field of view. CBCT scans were acquired during free breathing with a kV x-ray imaging system mounted on a Synergy[®] linear accelerator (Elekta AB, Stockholm, Sweden). Although intra-patient consistency was maintained, there were minor variations between patients in the following parameters: tube current (40 mA in 20 patients; 25 mA in 3 patients), exposure time (40 ms in 20 patients; 10 ms in 3 patients) and slice thickness (3 mm in 20 patients; 1 mm in 3 patients). Overall survival was defined as the time from the first day of treatment until death from any cause. Patients that were alive at the last known follow-up were censored.

GTV propagation

Figure 1 illustrates the schematic of the analysis performed in the study. The first step was to propagate the gross tumor volume (GTV) contours from the planning CT image to the CBCT images using deformable image registration (DIR). The GTV, defined as the primary tumor and regionally involved lymph nodes identified on



the planning CT image, was contoured for clinical treatment planning. DIR was performed between the planning CT image (fixed) and CBCT image of the first fraction (moving), and then between the two consecutive CBCT images using the hybrid DIR algorithm (without setting controlling structures) of the RayStation treatment planning system (RaySearch Laboratories AB, Stockholm, Sweden) (Weistrand and Svensson 2015). The accuracy of this algorithm for contour propagation has been validated with thorax CT image datasets in a multi-institutional study (Loi *et al* 2018). Dice similarity coefficients were >0.85 for the spatial overlap between the DIR-propagated contours and reference contours. The same level of accuracy was assumed in this study, and only visual inspection was performed to check for major errors.

Radiomics feature extraction

The second step was to extract radiomics features from each CBCT image dataset with the propagated GTV contour (figure 1). A total of 658 radiomics features (categorized into shape, intensity, texture and Laplacian of Gaussian (LoG) filter) were extracted using an open source software tool, IBEX (Aerts *et al* 2014, Zhang *et al* 2015). Shape features include the volume and surface area. Intensity features include intensity histogram features and first order statistical features derived directly from the image intensity. Texture features are calculated based on gray-level co-occurrence matrix (GLCM) (at different directions, yielding different values treated independently), gray-level run length matrix (GLRLM) (at different directions, yielding different values that were treated independently) and neighborhood intensity difference matrix (NIDM). LoG filter features are determined by applying LoG filters (with three filter parameters: size = 5, sigma = 1; size = 7, sigma = 1.5; and size = 11, sigma = 2.5, yielding three different values that were treated independently) to the image dataset, then calculating the first order statistical features. For texture features, all image datasets were rescaled into an 8-bit depth to reduce the effect of image noise and prevent sparsely populated matrices from being produced. Intensity features were calculated both with and without 8-bit depth rescaling, yielding two different values for a given feature, which were treated as two independent features. No image resampling was performed.

Radiomics feature selection

The third step was to select radiomics features for the data analysis (figure 1). Selection criteria included: ‘test–retest’ repeatability, robustness against contouring uncertainties, and non–redundancy. For the repeatability, we quantified the intraclass correlation coefficient (ICC) (2,1) (for the absolute agreement among measurements) between pairs of feature values extracted from the CBCT image datasets of the first two treatment fractions (assuming negligible changes in response to treatment) using 15 patients. From the same cohort of 67 patients with stage III NSCLC mentioned above, we selected 15 patients who underwent CBCT imaging on the first

two fractions with the same imaging parameters (tube voltage 120 kVp, current 40 mA, exposure time 40 ms, and slice thickness 3 mm) as those of the majority of CBCT images used for the analysis (220 of all 253 CBCT images for 20 of 23 patients). The rationale is to approximate conditions required for the evaluation of test–retest repeatability by eliminating differences in imaging parameters between the two CBCT images. For the robustness, we quantified the ICC(2,1) between pairs of feature values extracted from the planning CT images with two distinct GTV contours delineated previously by two different radiation oncologists for another study using a separate dataset of 15 patients with stage III NSCLC. These 15 patients were among 67 patients reviewed in this study but independent from those used for the analysis. The mean Dice similarity coefficient for the spatial overlap between the two contours was 0.68 (standard deviation: 0.18). Features with an ICC > 0.9 for both the repeatability and robustness were identified, and then evaluated for the redundancy using the CBCT image datasets of the first fraction of the same 15 patients used for the repeatability. We calculated the Spearman’s correlation coefficient (r_s) between different pairs of features. If the r_s was >0.8, the one with higher repeatability was selected for the subsequent analysis.

Characterizing changes in radiomics features during treatment

For the first part of data analysis, we characterized changes in CBCT-based radiomics features during treatment. All feature values were normalized to the baseline value. We also explored whether CBCT-based features early during treatment can predict features at the end of treatment. Linear models were fitted using all the features between the first and k th ($k = 4, 7, 10, \dots$) fractions, and then were used to predict the feature at the end of treatment. The coefficient of determination (R^2) for the relationship between the predicted and actual values at the end of treatment was quantified as a measure of the predictive ability. We evaluated how the predictive ability varied with k .

Prediction of overall survival

For the second part of data analysis, we quantified the predictive ability of CBCT-based delta-radiomics features for overall survival using two methods. The delta-radiomics feature $|\Delta\text{Feature}_{(1:k)}|$ at the k th fraction was defined by

$$|\Delta\text{Feature}_{(1:k)}| = \left| \frac{3}{k-1} \sum_{\substack{m=3n+1 \\ n \in \{1, 2, 3, \dots\}}}^k \frac{\text{Feature}_m - \text{Feature}_1}{\text{Feature}_1} \right|$$

where Feature_m is the feature value at the m th fraction. Firstly, we compared the delta-radiomics features between two groups of patients divided by a cutoff survival time of 18 months. The 18-month survival time is considered clinically relevant in locally advanced NSCLC and consistent with cutoff times used in previous studies (range 12–24 months) (Hoang *et al* 2005, Oberije *et al* 2014). The Kolmogorov–Smirnov test was used to test data normality. We used the two-sided t -test for the normally distributed data and the two-sided Wilcoxon rank-sum test for the non-normally distributed data to investigate whether the difference was statistically significant at different time points (k). Secondly, we calculated Kaplan–Meier overall survival curves of two groups of patients divided by the median of the delta-radiomics feature, and used the log-rank test to quantify the univariate discrimination of the two groups. Multiple testing correction was applied to all the results based on the false discovery rate (FDR) procedure, (Benjamini and Hochberg 1995, Storey 2002) where a q -value less than 0.05 was considered statistically significant.

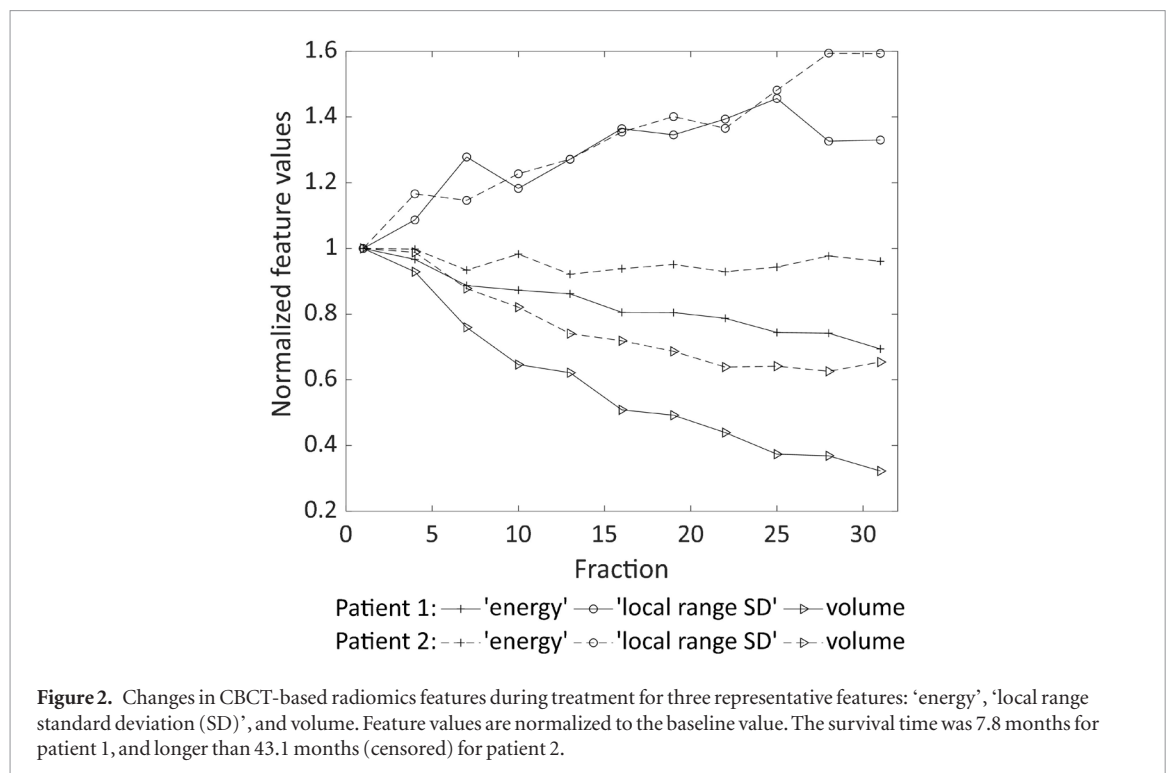
Results

Feature selection

Of 658 radiomics features calculated in this study, 474 features met the repeatability criteria. Of 474 features, 301 features met the robustness criteria. Finally, the following seven features met the redundancy criteria: volume; ‘0.75 quantile’ (without 8-bit rescaling); ‘global max’ (with 8-bit rescaling); ‘local range standard deviation (SD)’ (with 8-bit rescaling), ‘energy’; ‘inverse difference normalized (IDN)’, and ‘65 percentile’ (LoG filter feature). Supplementary table 2 shows details of these features.

Changes in radiomics features during treatment

Figure 2 shows changes in three representative CBCT-based radiomics feature (‘energy’, ‘local range SD’, and volume) during treatment for two representative patients. The survival time was 7.8 months for patient 1, and >43.1 months (censored) for patient 2. Changes in all the three features presented a clear time trend. The



rates of changes in ‘energy’ and volume were greater in patient 1 than in patient 2, while that of ‘local range SD’ was similar between the two patients. Changes in the other four features for the two patients are shown in supplementary figures 1–4.

Features early during treatment were predictive of features at the end of treatment (i.e. $R^2 > 0.64$ for the relationship between the predicted and actual feature values) for all the seven features. Figure 3 shows the R^2 as a function of the fraction number (k) used for prediction. The R^2 generally increased with increasing k as expected. There were considerable differences between the features in the earliest predictive time point, ranging from the 10th fraction (‘energy’, ‘IDN’, ‘0.75 quantile’, and volume) to the 22nd fraction (‘global max’) and 28th fraction (‘local range SD’ and ‘65 percentile’).

Prediction of overall survival

Figure 4 shows q -values for the differences of the delta-radiomics features between the two groups of patients as a function of the fraction number (k) used to calculate the delta-radiomics features. The FDR step-up procedure resulted in some identical q -values in consecutive time points, e.g. ‘energy’ after the 16th fraction. Two texture features (‘energy’ and ‘IDN’) and ‘0.75 quantile’ were predictive of overall survival as early as the 10th, 13th and 19th fractions, respectively. The remaining four features were not predictive at any fractions. For the three predictive features, delta-radiomics feature values were greater in patients with shorter survival time than in those with longer survival time (figure 5). Patients’ clinical characteristics and imaging parameters were comparable between the two groups of patients.

According to the log-rank statistics, only ‘energy’ and ‘IDN’ were predictive of survival. Q -values generally decreased with increasing k . Both ‘energy’ and ‘IDN’ were predictive of survival as early as the 10th fraction (table 1). Figure 6 shows comparisons of Kaplan–Meier overall survival curves between two groups of patients stratified by the median of $|\Delta \text{energy}|_{(1:10)}$ and the median of $|\Delta \text{volume}|_{(1:10)}$. ‘Energy’ significantly discriminated between patients with higher and lower survival probabilities ($q < 0.01$), whereas the volume did not show significant discriminatory power ($q = 0.12$).

Discussion

To the best of our knowledge, this is the first study correlating CBCT-based delta-radiomics features with clinical outcomes. We demonstrated a significant association between CBCT-based delta-radiomics features (‘energy’ and ‘IDN’) and overall survival in locally advanced NSCLC. These features were found to be predictive of survival as early as the 10th fraction of treatment. Our findings provide preliminary evidence for the prognostic value of CBCT-based delta-radiomics for early response assessment in lung cancer. Also, we demonstrated a strong relationship between the features at the end of treatment predicted by fitting a linear model to the features early

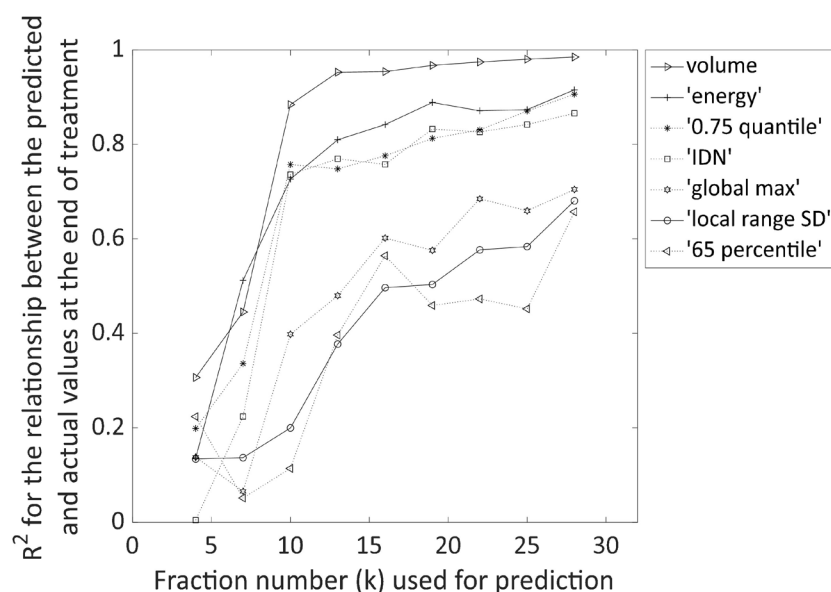


Figure 3. The coefficient of determination (R^2) for the relationship between the predicted and actual values at the end of treatment as a function of the fraction number (k) used for prediction for the selected seven features.

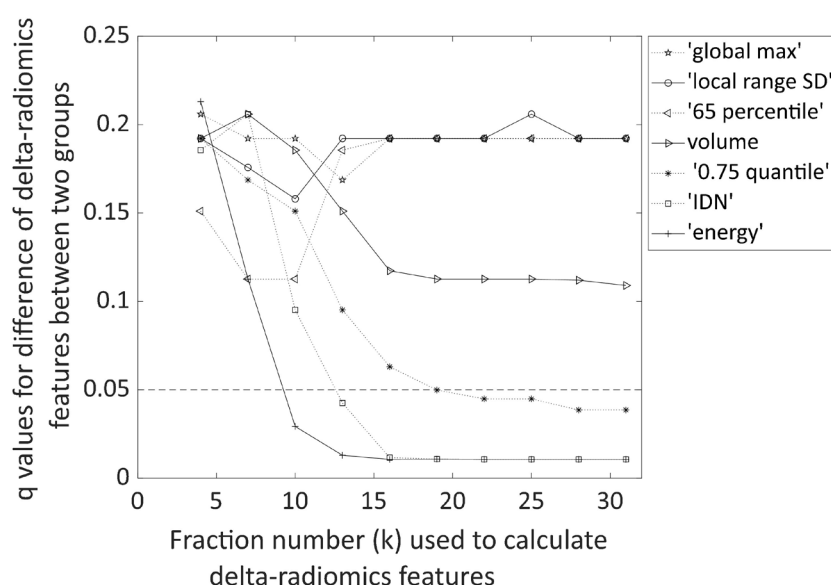


Figure 4. Q-values for the differences of delta-radiomics features ($|\Delta \text{Feature}_{(1:k)}|$) between the two groups of patients divided by a cutoff survival time of 18 months as a function of the fraction number (k) used to calculate delta-radiomics features for the selected seven features. $Q < 0.05$ (the dashed line) was considered statistically significant.

during treatment and the actual feature, suggesting that CBCT-based radiomics features can be described by a simple linear model. Previous studies have also demonstrated the association of delta-radiomics based on other modalities (including CT and ^{18}F -FDG PET) with clinical outcomes in lung cancer (Carvalho *et al* 2016, Dong *et al* 2016, Fave *et al* 2017). Van Timmeren *et al* found that CBCT-based delta-radiomics features were detectable as early as the second week of treatment in NSCLC (van Timmeren *et al* 2017a), which is in line with our findings that the 10th fraction of treatment (corresponding to the second week) was the earliest time point predictive of features at the end of treatment as well as overall survival.

We did not find a significant association between tumor volume changes and survival. Previous studies have reported inconsistent, conflicting data on the association of tumor volume changes with clinical outcomes. Some studies have reported no significant association with survival (Willner *et al* 2002, Carvalho *et al* 2016), which is consistent with this study. Other studies have found a significant association with survival (Bral *et al* 2011, Brink *et al* 2014, Jabbour *et al* 2015, Mazzola *et al* 2016, Wen *et al* 2017); however, conflicting findings have been reported as described in the Introduction (Brink *et al* 2014, Jabbour *et al* 2015). Further studies are needed to investigate

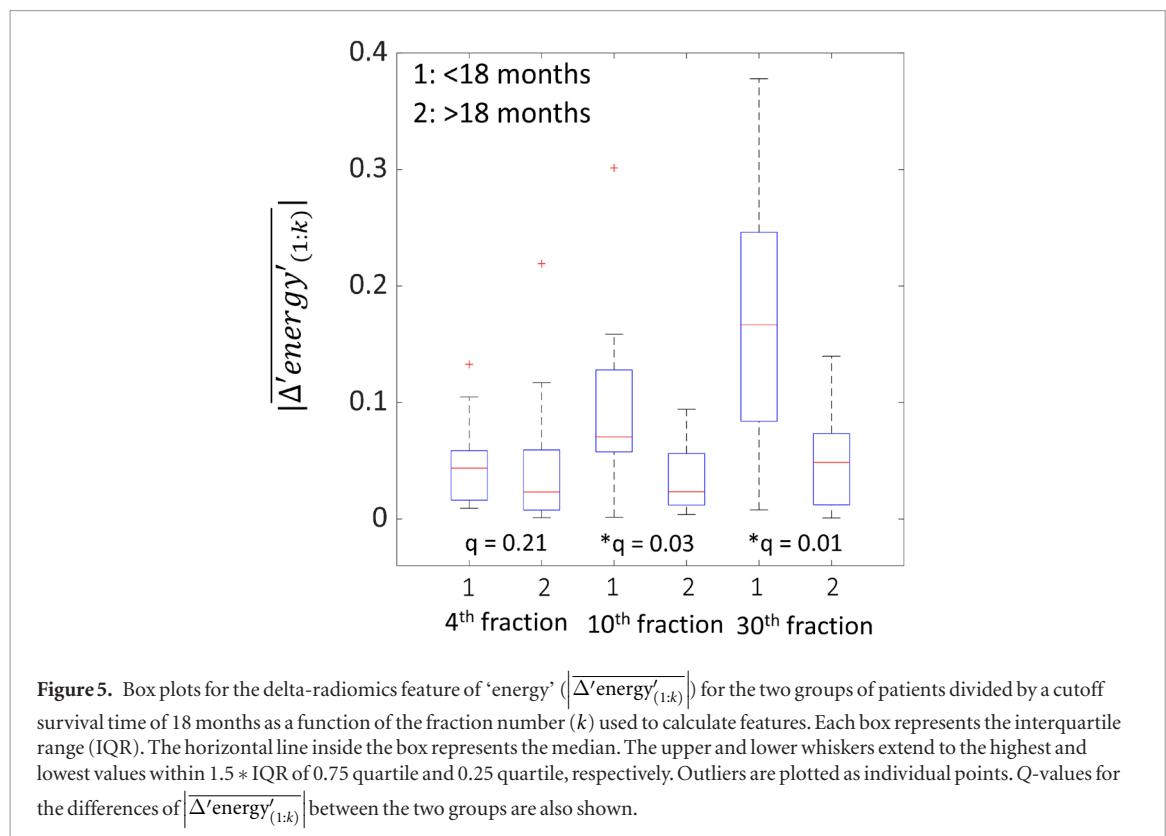


Table 1. Log-rank q -values for the univariate discrimination of overall survival by the median of seven selected delta-radiomics features.

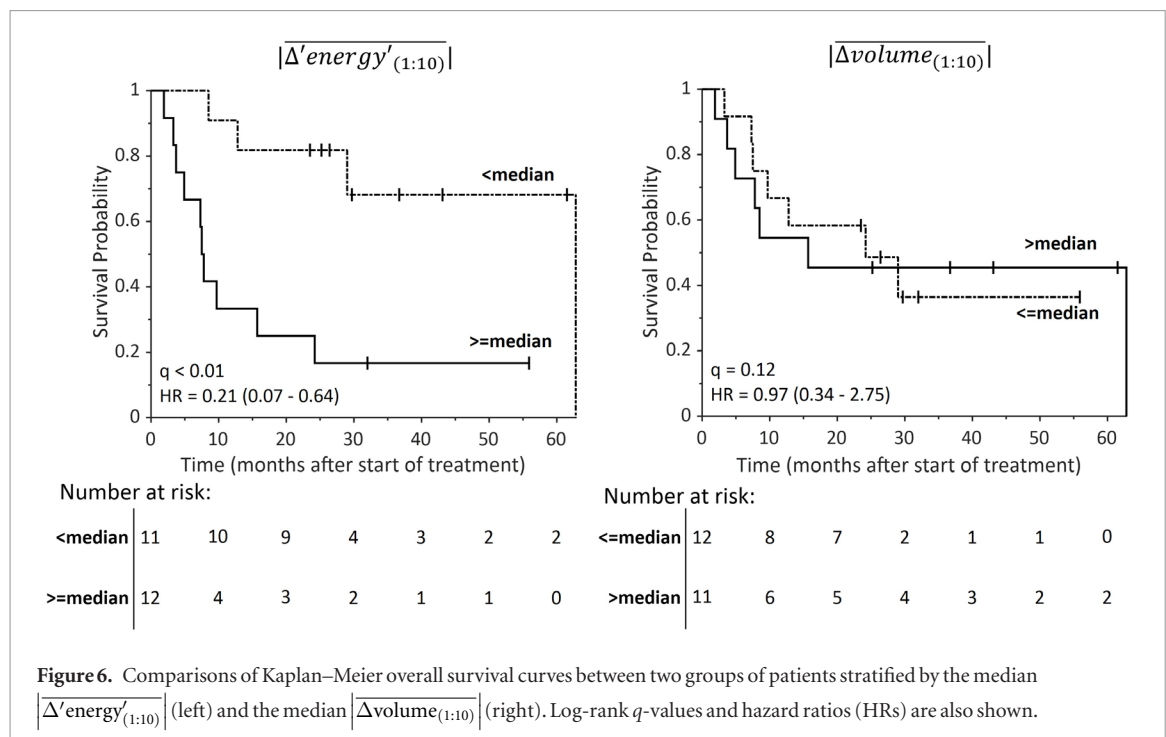
Fraction number (k)	Texture features			Intensity features		LoG feature	Shape feature
	'Energy'	'IDN'	'Global max'	'Local range SD'	'0.75 quantile'	'65 percentile'	Volume
4	0.09	0.07	0.09	0.09	0.12	0.06	0.09
7	0.05	0.12	0.11	0.07	0.10	0.02	0.14
10	< 0.01	0.02	0.10	0.06	0.10	0.05	0.12
13	< 0.01	0.05	0.13	0.03	0.09	0.05	0.12
16	< 0.01	0.02	0.11	0.05	0.09	0.08	0.12
19	0.01	0.05	0.09	0.09	0.09	0.12	0.05
22	0.04	< 0.01	0.09	0.11	0.07	0.12	0.09
25	< 0.01	< 0.01	0.09	0.11	0.10	0.12	0.05
28	< 0.01	< 0.01	0.09	0.11	0.10	0.11	0.05
30	< 0.01	< 0.01	0.09	0.13	0.12	0.11	0.05

Abbreviation: IDN: inverse difference normalized; SD: standard deviation; LoG: Laplacian of Gaussian.

Italic $q < 0.05$.

the prognostic values of tumor volume changes in lung cancer (Mattonen *et al* 2014, Zayed and Elnemr 2015, Mattonen *et al* 2016).

An interesting observation from this study is that patients with smaller delta-radiomics features (i.e. smaller changes) are associated with better survival. This may seem counterintuitive; however, similar findings have been previously observed with tumor volume changes measured with CBCT (Brink *et al* 2014), tumor metabolism measured with FDG PET (van Baardwijk *et al* 2007), and tumor proliferation measured with $3'$ - ^{18}F -fluoro- $3'$ -deoxy-L-thymidine (^{18}F -FLT) PET (Bradshaw *et al* 2015). Brink *et al* showed that lung cancer patients with pronounced tumor volume regression during treatment had worse survival (Brink *et al* 2014). Bradshaw *et al* reported that patients with large reductions in FLT uptake during radiotherapy had a shorter time to progression than those with small changes or increases in FLT uptake using a canine model with nasal tumors (Bradshaw *et al* 2015). One explanation for these counterintuitive findings is that tumors with pronounced response early during treatment might indicate the aggressiveness of the tumor and could be more likely to regrow rapidly after treatment, leading to worse outcomes. Further studies are needed to investigate underlying mechanisms.



The low image quality due to substantial scatter is one of the main disadvantages of CBCT. Nevertheless, Fave *et al* demonstrated that some CBCT-based radiomics features were robust to the image noise and poor image quality (Fave *et al* 2015). Van Timmeren *et al* showed that some radiomics features extracted from CT and CBCT were interchangeable (van Timmeren *et al* 2017b). These results as well as our findings suggest the potential for CBCT-based delta-radiomics to serve as an early imaging biomarker to predict clinical outcomes.

In this study, we calculated delta-radiomics features based on the mean change between the first and k th fractions rather than the change at each time point used in a previous delta-radiomics study (Fave *et al* 2017). Delta-radiomics features based on the change at each time point yielded larger fluctuations in the q -values over time and generally larger q -values compared to those of delta-radiomics features based on the mean change (supplementary figure 5). One likely explanation is that the delta-radiomics based on the change at each time point uses smaller datasets and hence more susceptible to image noise, leading to larger uncertainties.

There are several limitations to this study. First, the sample size is small, and hence the findings of this study should be considered preliminary. Further studies are necessary to validate the models through a large-scale study with appropriate approaches such as strategies described in the Transparent Reporting of a multivariable prediction model for Individual Prognosis Or Diagnosis (TRIPOD) statement (Collins *et al* 2015). Second, only visual inspection was performed to check the accuracy of DIR, assuming the same level of accuracy as previous studies. However, we consider the effect of residual DIR errors on the results to be small because radiomics features were selected using the robustness against contouring uncertainties as one of the criteria, which implicitly accounts for uncertainties in DIR as well. Third, respiratory motion, which was previously found to have a considerable effect on the repeatability of CBCT-based radiomics features, was not directly accounted for in patient selection. However, we selected features using the ‘test–retest’ repeatability quantified with 15 patients of the 23 eligible patients, including tumors in the lower lobe, thus the effect of motion on the results may be minimal. Fourth, we only fitted a linear model using features early during treatment to predict the features at the end of treatment. The rationale is to avoid overfitting, especially given small datasets used for prediction in this study. Nevertheless, non-linear models might result in a better fit, and further studies are needed.

Conclusion

CBCT-based delta-radiomics features early during a course of treatment may be associated with overall survival in locally advanced NSCLC. Further large-scale studies are needed to validate these preliminary findings.

Acknowledgments

This study was supported in part by the China National Key Research and Development Program (2016YFC0103400) (LS and JQ) and Taishan Scholars Program of Shandong Province (LS and JQ). Dr Kun Hou at Taishan Medical University provided writing assistance. Dr Weizhao Lu and Dr Dong Cui at Taishan Medical

University provided assistance in statistical analysis. Dr Wen Chen at University of California Davis assisted with CBCT image analysis.

Conflicts of interest

None.

ORCID iDs

Yi Rong  <https://orcid.org/0000-0002-2620-1893>

Tokihiro Yamamoto  <https://orcid.org/0000-0002-6790-6523>

References

- Aerts H J *et al* 2014 Decoding tumour phenotype by noninvasive imaging using a quantitative radiomics approach *Nat. Commun.* **5** 4006
- Benjamini Y and Hochberg Y 1995 Controlling the false discovery rate: a practical and powerful approach to multiple testing *J. R. Stat. Soc. B* **57** 289–300
- Bradshaw T J, Bowen S R, Deveau M A, Kubicek L, White P, Bentzen S M, Chappell R J, Forrest L J and Jeraj R 2015 Molecular imaging biomarkers of resistance to radiation therapy for spontaneous nasal tumors in canines *Int. J. Radiat. Oncol. Biol. Phys.* **91** 787–95
- Bral S, De Ridder M, Duchateau M, Gevaert T, Engels B, Schallier D and Storme G 2011 Daily megavoltage computed tomography in lung cancer radiotherapy: correlation between volumetric changes and local outcome *Int. J. Radiat. Oncol. Biol. Phys.* **80** 1338–42
- Brink C, Bernchou U, Bertelsen A, Hansen O, Schytte T and Bentzen S M 2014 Locoregional control of non-small cell lung cancer in relation to automated early assessment of tumor regression on cone beam computed tomography *Int. J. Radiat. Oncol. Biol. Phys.* **89** 916–23
- Carvalho S, Leijenaar R T H, Troost E G C, van Elmpt W, Muratet J P, Denis F, De Ruyscher D, Aerts H J W L and Lambin P 2016 Early variation of FDG-PET radiomics features in NSCLC is related to overall survival—the ‘delta radiomics’ concept *Radiother. Oncol.* **118** S20–S1
- Collins G S, Reitsma J B, Altman D G and Moons K G M 2015 Transparent reporting of a multivariable prediction model for individual prognosis or diagnosis (TRIPOD): the TRIPOD statement *Ann Intern Med.* **162** 55–63
- Dong X *et al* 2016 Early change in metabolic tumor heterogeneity during chemoradiotherapy and its prognostic value for patients with locally advanced non-small cell lung cancer *PLoS One* **11** e0157836
- Dubben H H, Thames H D and Beckbornholdt H P 1998 Tumor volume: a basic and specific response predictor in radiotherapy *Radiother. Oncol.* **47** 167–74
- Fave X *et al* 2015 Can radiomics features be reproducibly measured from CBCT images for patients with non-small cell lung cancer? *Med. Phys.* **42** 6784
- Fave X *et al* 2017 Delta-radiomics features for the prediction of patient outcomes in non-small cell lung cancer *Sci. Rep.* **7** 588
- Guckenberger M, Wilbert J, Richter A, Baier K and Flentje M 2011 Potential of adaptive radiotherapy to escalate the radiation dose in combined radiochemotherapy for locally advanced non-small cell lung cancer *Int. J. Radiat. Oncol. Biol. Phys.* **79** 901–8
- Hoang T, Xu R, Schiller J H, Bonomi P and Johnson D H 2005 Clinical model to predict survival in chemonaive patients with advanced non-small-cell lung cancer treated with third-generation chemotherapy regimens based on Eastern Cooperative Oncology Group Data *J. Clin. Oncol.* **23** 175–83
- Huynh E, Coroller T P, Narayan V, Agrawal V, Hou Y, Romano J, Franco I, Mak R H and Aerts H J 2016 CT-based radiomic analysis of stereotactic body radiation therapy patients with lung cancer *Radiother. Oncol.* **120** 258–66
- Jabbour S K *et al* 2015 Reduction in tumor volume by cone beam computed tomography predicts overall survival in non-small cell lung cancer treated with chemoradiation therapy *Int. J. Radiat. Oncol. Biol. Phys.* **92** 627–33
- Kumar V *et al* 2012 Radiomics: the process and the challenges *Magn. Reson. Imaging* **30** 1234–48
- Kupelian P A, Ramsey C, Meeks S L, Willoughby T R, Forbes A, Wagner T H and Langen K M 2005 Serial megavoltage CT imaging during external beam radiotherapy for non-small-cell lung cancer: observations on tumor regression during treatment *Int. J. Radiat. Oncol. Biol. Phys.* **63** 1024–8
- Lambin P *et al* 2012 Radiomics: extracting more information from medical images using advanced feature analysis *Eur. J. Cancer* **48** 441–6
- Loi G *et al* 2018 Performance of commercially available deformable image registration platforms for contour propagation using patient-based computational phantoms: a multi-institutional study *Med. Phys.* **45** 748–57
- Mattonen S A, Palma D A, Haasbeek C J, Senan S and Ward A D 2014 Early prediction of tumor recurrence based on CT texture changes after stereotactic ablative radiotherapy (SABR) for lung cancer *Med. Phys.* **41** 033502
- Mattonen S A *et al* 2016 Detection of local cancer recurrence after stereotactic ablative radiation therapy for lung cancer: physician performance versus radiomic assessment *Int. J. Radiat. Oncol. Biol. Phys.* **94** 1121–8
- Mazzola R, Fiorentino A, Ricchetti F, Gaj Levra N, Fersino S, Di Paola G, Lo Casto A, Ruggieri R and Alongi F 2016 Cone-beam computed tomography in lung stereotactic ablative radiation therapy: predictive parameters of early response *Br. J. Radiol.* **89** 20160146
- Molina J R, Yang P, Cassivi S D, Schild S E and Adjei A A 2008 Non-small cell lung cancer: epidemiology, risk factors, treatment, and survivorship *Mayo Clin. Proc.* **83** 584
- Mozley P D, Bendtsen C, Zhao B, Schwartz L H, Thorn M, Rong Y, Zhang L, Perrone A, Korn R and Buckler A J 2012 Measurement of tumor volumes improves RECIST-based response assessments in advanced lung cancer *Transl. Oncol.* **5** 19–25
- Oberije C *et al* 2014 A prospective study comparing the predictions of doctors versus models for treatment outcome of lung cancer patients: a step toward individualized care and shared decision making *Radiother. Oncol.* **112** 37–43
- Smith R A, Andrews K S, Brooks D, Fedewa S A, Manassaram-Baptiste D, Saslow D, Brawley O W and Wender R C 2018 Cancer screening in the United States, 2018: a review of current American Cancer Society guidelines and current issues in cancer screening *CA Cancer J. Clin.* **68** 297–316
- Storey J D 2002 A direct approach to false discovery rates *J. R. Stat. Soc. B* **64** 479–98
- van Baardwijk A *et al* 2007 Time trends in the maximal uptake of FDG on PET scan during thoracic radiotherapy. A prospective study in locally advanced non-small cell lung cancer (NSCLC) patients *Radiother. Oncol.* **82** 145–52

- van Timmeren J E, Leijenaar R T H, van Elmpt W, Reymen B and Lambin P 2017a Feature selection methodology for longitudinal cone-beam CT radiomics *Acta Oncol.* **56** 1537–43
- van Timmeren J E, Leijenaar R T H, van Elmpt W, Reymen B, Oberije C, Monshouwer R, Bussink J, Brink C, Hansen O and Lambin P 2017b Survival prediction of non-small cell lung cancer patients using radiomics analyses of cone-beam CT images *Radiother. Oncol.* **123** 363–9
- Weistrand O and Svensson S 2015 The ANACONDA algorithm for deformable image registration in radiotherapy *Med. Phys.* **42** 40–53
- Wen Q, Zhu J, Meng X, Ma C, Bai T, Sun X and Yu J 2017 The value of CBCT-based tumor density and volume variations in prediction of early response to chemoradiation therapy in advanced NSCLC *Sci. Rep.* **7** 14650
- Willner J, Baier K, Caragiani E, Tschammler A and Flentje M 2002 Dose, volume, and tumor control prediction in primary radiotherapy of non-small-cell lung cancer *Int. J. Radiat. Oncol. Biol. Phys.* **52** 382–9
- Zayed N and Elnemr H A 2015 Statistical analysis of Haralick texture features to discriminate lung abnormalities *Int. J. Biomed. Imaging* **2015** 267807
- Zhang L, Fried D V, Fave X J, Hunter L A, Yang J and Court L E 2015 IBEX: an open infrastructure software platform to facilitate collaborative work in radiomics *Med. Phys.* **42** 1341–53